Environmental Science and Pollution Research (2020) 27:32017–32033
https://doi.org/10.1007/s11356-020-08916-9

RESEARCH ARTICLE

Antiproliferative and apoptogenic effects of *Cassia fistula* L. n-hexane fraction against human cervical cancer (HeLa) cells

Sandeep Kaur[1,2] · Kritika Pandit[1] · Madhu Chandel[2] · Satwinderjeet Kaur[1]

Received: 8 September 2019 / Accepted: 16 April 2020 / Published online: 6 June 2020

Abstract

The current study was performed to evaluate the antiproliferative and apoptosis-inducing potential of n-hexane fraction from *Cassia fistula* L. (Caesalpinioideae) fruits. The antiproliferative property of the fraction was determined by MTT assay against cancer cell lines including HeLa, MG-63, IMR-32, and PC-3 with GI_{50} value of 97.69, 155.2, 143, and 160.2 μg/ml respectively. The fraction was further explored for its apoptotic effect using confocal, SEM, and flow cytometry studies in HeLa cells. It was observed that the treatment of fraction revealed fragmentation of DNA, chromatin condensation, membrane blebbing, and formation of apoptotic bodies in a dose-dependent manner. The fraction also showed a remarkable increase in the level of ROS, mitochondrial depolarization and G_0/G_1 phase cell cycle arrest, and induction in the phosphatidylserine externalization analyzed using Annexin V-FITC/PI double staining assay in HeLa cells. Kaempferol, Ellagic acid, and Epicatechin are the major phytoconstituents present in the fraction as revealed by the HPLC. The treatment of n-hexane fraction showed downregulation in the gene expression of Bcl-2 and upregulation in the expression level of p53, Bad, and caspase-3 genes analyzed using semi-quantitative RT-PCR in HeLa cells. These results suggest that n-hexane fraction from *C. fistula* inhibited the proliferation of cervical cancer cells efficiently by the induction of apoptosis.

Keywords *Cassia fistula* · Antiproliferative · Apoptosis · HeLa cells · HPLC

Introduction

Cancer is a multifactorial disease and is characterized by unregulated growth, dysregulation of cell signaling pathways, and dissemination of malignantly transformed neoplastic cells (Salehi et al. 2018; Rather and Bhagat 2018). It remains the plague of the century as it is still the major cause of morbidity and mortality worldwide, which accounts for 14 million new cases and roughly 8 million deaths each year (Torre et al. 2015; Kotecha et al. 2016; Muntean et al. 2018). The quintessential traits of cancer cells involve insensitivity to antigrowth signals, self-sufficiency in growth signals, sustained angiogenesis, evasion of apoptosis, tissue invasion, limitless replicative potential, and metastasis which collectively dictate the conversion and/or transformation of a normal cell to a malignant phenotype (Hanahan and Weinberg 2000; Priyadarsini and Nagini 2012). The cancer development process undergoes several stages of genetic and biochemical alterations in a target cell. Carcinogenesis is a multistep process that involves three discernible stages: initiation, promotion, and progression (Shu et al. 2010).

Cervical carcinoma is considered as the second most common and lethal gynecologic malignancy than breast cancer in women (Saei Ghare Naz et al. 2018). It was found that although many patients have been benefitted from chemoradiotherapy and surgery, the metastasis and recurrence rates remain high and ultimately lead to death (Yessaian et al. 2004; Chen et al. 2019). The radiotherapy treatment was applied to nearly 70% of cancer patients and regarded as the standard treatment for advanced malignancy of cervical cancer (Zhang et al. 2020).

Research directed toward elucidating underlying molecular mechanisms of chemoprevention with medicinal and dietary phytochemicals has recognized components of upregulation

Responsible editor: Mohamed M. Abdel-Daim

✉ Satwinderjeet Kaur
sjkaur.gndu@gmail.com; sjkaur2011@gmail.com

[1] Department of Botanical and Environmental Sciences, Guru Nanak Dev University, Amritsar, Punjab 143005, India

[2] Post Graduate Department of Botany, Khalsa College, Amritsar, India

of genes involved in cytoprotection that encode for detoxification/elimination of carcinogens and their reactive metabolites, repairing DNA damage, enhancing the immune system of the host, sensitizing malignant cells to cytotoxic agents, and modulating signal transduction pathways as potential targets (Neergheen et al. 2010; Kotecha et al. 2016). To date, much of the research has focused on the investigation of plant extracts and its bioactive phytoconstituents as effective therapeutic and prophylactic agents since they are capable of acting on specific and/or multiple cellular and molecular targets. Plants have been an abundant source of several highly effective phytochemicals that have gained significant recognition in the potential management of several human clinical conditions (Neergheen et al. 2010). Interestingly, extensive study in the field of traditional medicinal plants has recognized that secondary metabolites which act as a natural defense system for the host plant represent one of the major sources of compounds with antioxidant, antimutagenic, and chemopreventive properties (Reyes-Lopez 2005; Carino-Cortes et al. 2007).

In the Indian traditional medicine, *Cassia fistula* has been recommended for the treatment of various diseases. According to the Unani and Ayurvedic system of medicine, it is also called Aragwadha, meaning disease killer, and all the parts of the plant are useful in curing various ailments. The stem bark possesses antidysenteric properties, useful against chest pain, swelling, and skin complaints (Inkabi et al. 2017). Flowers and pods are used as febrifugal, purgative, biliousness, and astringent (Bhalerao and Kelkar 2012). The fruit pulp is found useful in urinary disorders, colic, and constipation and is a safe purgative for expectant mothers and children (Gupta and Jain 2009). Duraipandiyan et al. (2012) reported the cytotoxic and apoptosis-inducing potential of Rhein isolated from *Cassia fistula* L. flower in human colon adenocarcinoma COLO 320 DM cell line. Gomes et al. (2019) investigated the antiproliferative and cell cycle arresting potential of *Annona coriacea* Mart. fractions in cisplatin-resistant cell lines, SiHa and HeLa. It was found that the treatment of fractions inhibited the autophagic flow by the G2/M cell cycle arrest and an increase in the level of p21. It was evaluated that the chloroform fraction of *Rasagenthi Mezhugu* showed potent cytotoxic and apoptosis-inducing effects toward HPV-positive cervical cancer cells, ME-180 and SiHa (Riyasdeen et al. 2012). Preethy and co-workers (Preethy et al. 2012) reported the antiproliferative, cell cycle arrest, mitochondrial membrane depolarization, and early apoptosis-inducing properties of n-hexane and chloroform extracts of *Anisomeles malabarica* in HPV16-positive cervical cancer cells. A study has found that the four abietane diterpenoids were identified in the hexane extract from the roots of *Salvia sahendica* Boiss. & Buhse which showed more cytotoxicity against human cervical cancer (HeLa) cells than colorectal adenocarcinoma (Caco-2) cells (Moradi-Afrapoli et al. 2018).

Taking into consideration the traditional importance of medicinal plants, the current study was designed to unravel the potential of n-hexane fraction from *C. fistula* fruits for its antiproliferative and apoptosis-inducing mechanisms in human cervical cancer (HeLa) cell line.

Materials and methods

Chemicals and reagents

Hoechst 33342, Fluoromount, 2′,7′-dichlorodihydrofluorescein diacetate (DCFH-DA), Dulbecco's modified Eagle's medium (DMEM), paraformaldehyde, hexamethyldisilazane, glutaraldehyde, propidium iodide (PI), and Rhodamine-123 were obtained from Sigma (St. Louis, USA). Fetal bovine serum (FBS) was obtained from Biological Industries, USA. 3-(4,5-Dimethylthiazol-2-yl)-2,5-diphenyl tetrazolium bromide (MTT) and trypsin were purchased from HiMedia Pvt. Limited (Mumbai, India). Fluorescein isothiocyanate (FITC)-conjugated annexin V/PI assay (BD Pharmingen Annexin V-FITC apoptosis detection kit) and BD Cycletest plus DNA Kit were purchased from BD Biosciences, San Jose, USA. All the reagents used to carry out the experiments were of analytical (AR) grade.

Collection and authentication

The fruits of *C. fistula* were collected from the campus of Guru Nanak Dev University, Amritsar, Punjab (India) in the month of May. The authentication of the plant fruits and their botanical identification were made in the Herbarium of the Department of Botanical and Environmental Sciences, Guru Nanak Dev University, Amritsar and voucher specimens have been deposited in the Herbarium with accession No. 6781.

Extraction/fractionation of *C. fistula* fruits

The air-dried, cleaned, washed, and powdered *C. fistula* (1.5 kg) fruits were extracted with 80% methanol by using the maceration method and then filtered and concentrated it under reduced pressure using a Rota vapor (Buchi R-210, Switzerland) to yield 165 g of methanolic extract named as CaFM. Then, 300 ml of double-distilled water was added to CaFM extract which was further fractionated using separating funnel with different organic solvents in order of increasing polarity viz. hexane, chloroform, ethyl acetate, butanol, and distilled water to yield n-hexane fraction CaFH (0.27%), chloroform fraction CaFC (0.43%), ethyl acetate fraction CaFE (17.29%), n-butanol fraction CaFB (21.62%), and remaining aqueous fraction CaFA (24.32%) respectively. The polarities of the solvents were capable of partitioning and separating the secondary metabolites of the fractions as per their solubility (Flowchart I).

HPLC analysis and chromatographic conditions

The quantitative HPLC analysis of n-hexane fraction from *C. fistula* fruits was determined using Shimadzu UHPLC Nexera system (Shimadzu, MA, USA), equipped with a degasser and a quaternary pump (LC-30AD). The sample injection volume was 5 μl. An analytical column used was Enable C18 column (150 mm × 4.6 mm i.d. × 5 μm p.s.) also provided with the guard column (10 × 4 mm). The flow rate was constant at 1 ml/min and a total run time was 21 min. For chromatographic analysis, the continuous gradient of solvent A (0.1% acetic acid in water, pH 3) and solvent B (methanol) was used as elution of the mobile phase. The setting of gradient program was as follows: (0–12 min) 30% B, (12–16 min) 65% B, (16–18 min) 80% B, (18–19 min) 40% B, and (19–21 min) 30% B. The column oven (CTO-10AS) (Shimadzu, MA, USA) aids to maintain the constant temperature of 28 °C. The detection of data, delivery of solvent, and data processing were performed using Labsolutions software (version 5.09, Shimadzu, MA, USA). The photodiode array (PDA) detector (SPD-M20A) helps to monitor the chromatogram at 280 nm.

Cell culture

HeLa (human cervical cancer cells), MG-63 (human osteosarcoma), IMR-32 (human neuroblastoma), PC-3 (human prostate adenocarcinoma), and HL-7702 (normal human hepatocyte) cell lines were obtained from the National Centre for Cell Science (NCCS), Pune, India. The cells were maintained routinely for their proper growth and fresh medium was added periodically. The subculturing of the cells involves detachment of the cells from the substratum (growth surface) of the culture flask during the sub-confluent stage and then the fresh medium was added in new culture flasks to reinoculate the cells in it. HeLa, PC-3, IMR-32, MG-63, and normal cell line HL-7702 were cultured as a monolayer in DMEM (containing 10% FBS and antibiotic-antimycotic solution) and then incubated at 37 °C in a humidified atmosphere with 5% CO_2.

Cell viability was checked prior to experimentation using the method mentioned by Militao et al. (2006) with slight modifications. In this method, the cells were washed with 1× PBS and trypsinized followed by centrifugation at 1500 rpm for 5 min. The cell pellet obtained was suspended in fresh media and finally stained with Trypan blue dye (0.4% prepared in PBS) to calculate the number of unstained viable cells and stained non-viable cells. After calculating viability, cells were used to carry out different experiments.

MTT assay

The antiproliferative activity of the test sample was estimated as described by Mickisch et al. (1990) with slight modifications. The cells were cultured at the concentration of 1×10^4 cells/0.1 ml in 96-well microplates and allowed to adhere. After 24 h, the cells were treated using serial dilutions method with the different concentrations of the fraction. On the completion of another 24 h, 3-(4,5-dimethylthiazol-2-yl)-2,5-diphenyltetrazolium bromide (20 μl) was added in each well and incubated for 3 h and the viable cells were capable of reducing it into insoluble purple-colored formazan. Then the supernatant containing MTT solution was decanted from each well and finally the intracellular MTT formazan was dissolved in dimethyl sulfoxide (100 μl) for 5 min. The absorbance was read at 570 nm using a multiwell plate reader (BioTek Synergy HT).

$$\text{Cell viability} = (\text{OD}_{570} \text{ of treatment}/\text{OD}_{570} \text{ of control}) \times 100$$

The growth inhibition percentage was measured by the equation

$$\%\text{Growth inhibition} = 100 - \%\text{viability}$$

Flowchart I Isolation of extract/fractions from fruits of *Cassia fistula* L.

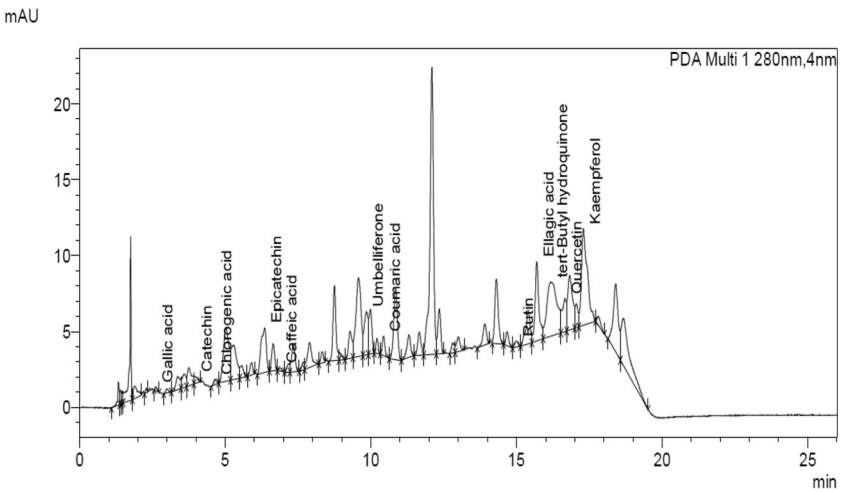

Lactate dehydrogenase assay

The cell membrane damage was determined by the lactate dehydrogenase (LDH) enzyme which is at the time of cell damage released rapidly and is present in all the cells. The assay was carried out to investigate cell death via necrosis as described by the method of Abe and Matsuki (2000). The cells were cultured at a density of 3.5×10^5 in 24-well plate for 24 h. Following incubation, the cells were treated with various concentrations of the sample calculated using MTT assay. After treatment, 100 μl of the supernatant obtained was collected and then transferred into a 96-well plate. After this, 100 μl of LDH buffer was added (2.5 mg NAD^+, 100 μl MTT, 2.5 mg Lithium lactate, Tris-HCl (pH 8.2) dissolved in Triton-X (0.1%), and 1 μl methoxyphenazine methosulfate). The mixture was incubated in dark for 30 min followed by the addition of 100 μl of 1 M acetic acid as a stop solution. The absorbance was measured at 570 nm using Biotek Synergy HT multi-well plate reader against blank and percentage enzymatic activity was expressed as:

$$\%\text{LDH activity} = (\text{OD}_{570} \text{ of treatment}/\text{OD}_{570} \text{ of control}) \times 100$$

Confocal microscopy

The cells were cultured at a density of 3.5×10^5 cells/well in a 6-well plate and a coverslip was placed in each well. After 24 h, the cells were treated with the test sample at different concentrations. After another 24 h, the cells' morphological features were observed under an inverted microscope. The media was decanted and the cells were washed twice with 1× PBS and fixed with paraformaldehyde (0.4%) for 10 min at ambient temperature. The cells were again washed thrice with 1× PBS followed by staining by the addition of Hoechst 33342 (5 μl) solution at 37 °C in dark for 20–30 min. Then, anti-fading reagent (Floromount, Sigma) was poured over the center of the slides and coverslip was put on it. Finally, the images were captured under a Nikon A1R Laser Scanning Confocal Microscope system (Nikon Corporation, Japan) using the software version 4.11.00 of NIS Elements AR analysis.

Scanning electron microscopy

Reactive oxygen species generation

The cells were cultured in a 6-well plate at a density of 4.8×10^5 cells/well for 24 h. After adherence, the cells were treated with the test sample at different concentrations for another 24 h. Then, the cells were trypsinized followed by centrifugation for 5 min at 2000 rpm. The cell pellet was obtained and washed twice with 1× PBS and again centrifuged. Further, the cells were incubated with DCFH-DA (10 μg/ml) for 20 min and harvested in the 15 ml conical tubes and centrifuged at 2000 rpm for 5 min. The cell pellet formed was washed twice with 1× PBS and centrifuged. Finally, the cell pellet obtained was suspended in 1× PBS (500 μl), and then analysis of the cell suspension was carried out by flow cytometry (BD Accuri C6 Flow Cytometer, BD Biosciences) with the help of BD Accuri software. The cell analysis was performed using the FL-1 channel (Emission λ 535 nm; excitation λ 488 nm).

Mitochondrial membrane potential ($\Delta\Psi m$)

The cells were cultured in a 6-well plate at a density of 4.8×10^5 cells/well for 24 h. On adherence, the cells were treated with the test sample at different concentrations for 24 h. After treatment, the media was removed and the cells were twice washed with 1× PBS followed by incubation with Rhodamine-123 (5 μg/ml) in the dark for 20 min. Further, the cells were harvested in falcon tubes and centrifuged at 2000 rpm for 5 min. After centrifugation, the supernatant obtained was discarded and the cell pellet was washed with 1× PBS. Again, the cells were centrifuged and the pellet obtained was suspended in 1× PBS (500 μl). Then, analysis of the cell suspension was carried out at flow cytometry (BD Accuri C6 Flow Cytometer, BD Biosciences) with the help of BD Accuri software. The cell analysis was performed using the FL-1 channel (Emission λ 535 nm; excitation λ 488 nm).

Cell-cycle phase distribution

The cell cycle phase distribution analysis in the cells treated with the sample was carried out using BD Cycletest plus DNA Kit (BD Biosciences). The cells were cultured in a 6-well plate at the density of 4.8×10^5 cells for adherence. After 24 h, cells were treated with the test sample at varying concentrations. On completion of treatment, both adhered and floating cells were collected in falcon tubes and centrifuged at 2000 rpm for 5 min. The cell pellet was washed twice with 1× PBS and centrifuged followed by the addition of 70% ethanol for fixing and kept at − 20 °C for 1 h. After fixation, the cell suspension was washed thrice with 1× PBS, added with 250 μl of solution A (trypsin buffer), and incubated each tube for 10 min at room temperature. Further, 200 μl of solution B (trypsin inhibitor and RNase buffer) was added and incubated for another 10 min followed by the addition of 200 μl of cold solution C (PI stain solution) and incubated in dark on ice for 1 h. Finally, the stained cells were analyzed by flow cytometry using BD Accuri software (BD Accuri C6 Flow Cytometer, BD Biosciences).

Annexin V-FITC/PI double staining

The apoptosis was evaluated in cells treated with a test sample using fluorescein isothiocyanate (FITC)-conjugated annexin V/PI assay (BD Pharmingen Annexin V-FITC apoptosis detection kit, Biosciences). The cells were cultured at a density of 4.8×10^5 in 6-well plates and allowed to adhere. After 24 h, cells were treated with the test sample at different concentrations. On completion of treatment, both adhered and floating cells were collected in tubes and centrifuged. The obtained cell pellets were washed thrice with 1× PBS, centrifuged, and then suspended in binding buffer (100 μl) for 15 min. Finally, Annexin V-FITC conjugate (5 μl) was added, followed by the addition of Propidium iodide (5 μl), and then incubated for 30 min in the dark. To this suspension, 400 μl of binding buffer was added. The stained cells were analyzed using BD Accuri software by flow cytometry (BD Accuri C6 Flow Cytometer, BD Biosciences).

Semi-quantitative RT-PCR

For the gene expression studies of various genes (Bcl-2, Bad, and p53 genes), semi-quantitative primers were designed: Bcl-2 (FP: 5′ AGTCTGGGAATCGATCTGGA 3′; RP: 5′ GGCAACGATCCCATCAATCT 3′) (T_m 52 °C), Bad (FP: 5′ TGGGGCTGTGGAGATCCG 3′; RP: 5′ GGAGTCCA CAAACTCGTCACT 3′) (T_m 54 °C), p53 (FP: 5′ TCACTGAAGACCCAGGTCCA 3′; RP: 5′ TTGGCTGT CCCAGAATGCAA 3′) (T_m 55 °C), and caspase-3 (FP: 5′ TCACAGCAAAAGGAGCAGTT 3′; RP: 5′ TGAAAAGT TTGGGTTTTCCAGTT 3′) (T_m 52 °C). Total RNA from the control and CaFH fraction-treated HeLa cells was extracted using the TRIzol method as per the manufacturer's instructions. A total of 1 μg of RNA was used for the cDNA preparation with a commercial cDNA synthesis kit (Bio-Rad) according to the manufacturer's protocol. Gene expression was studied in 20 μl of polymerase chain reaction (PCR) using 20 ng of cDNA template. The PCR parameters used were initial denaturation at 95 °C for 4 min, followed by 35 cycles of 95 °C for 1 min, (annealing temp.)°C for 1 min, 72 °C for 1 min (extension temp.), and a final extension step of 72 °C for 10 min. β-actin was used as an internal control. All the PCRs were performed at least with three independent samples and the intensity of the products was confirmed with 2% agarose gel with ethidium bromide.

Statistical analysis

For all the values, the statistical significance was calculated by one-way analysis of variance ANOVA (*F* test). The difference of the means was compared using a high range statistical domain (HSD) by Tukey's test. The regression equation obtained was calculated using Microsoft excel. The values in all the experiments were represented as mean ± standard errors in triplicate. The probability $p \leq 0.05$ demonstrated that the values obtained were statistically significant at a 5% level of significance.

Results

HPLC profiling

Kaempferol, Ellagic acid, and Epicatechin are the major phytoconstituents present in CaFH fraction as demonstrated by the HPLC profiling with the concentration of 38, 10.61, and 9.504 ppm respectively. The other phenolic constituents were detectable in very low concentrations. By applying the same parameters, 12 different standard polyphenolic compounds were run and the chromatogram was detected at 280 nm. The analysis of the bioactive compounds present in the CaFH fraction was carried out based on the retention time of the standard compounds (Table 1 and Fig. 1).

Antiproliferative activity

It was evident from the results that the cytotoxicity induced by CaFH fraction was stronger toward HeLa cancer cells with the GI_{50} of 97.69 μg/ml. We treated the human cervical cancer HeLa cells with CaFH (31.25–500 μg/ml) for 24 h and confirmed that the CaFH was effective in inhibiting the proliferation of cancer cells dose-dependently. The antiproliferative potential of a fraction against other cancer cell lines was found in the order of IMR-32 followed by MG-63 and PC-3 with the GI_{50} value of 143.06, 155.2, and 160.2 μg/ml respectively. In the case of a normal human hepatocyte HL-7702 cell line, the fraction was found to be ineffective and showed no toxicity as no significant difference was observed in the percentage growth inhibition. Therefore, CaFH exhibited a potent inhibitory effect toward the proliferation of human cervical cancer HeLa cells, with minimum cytotoxicity against normal cells (Fig. 2).

Lactate dehydrogenase assay

The cytotoxic effects were further investigated through the LDH release assay on human cervical cancer HeLa cells. The treatment of CaFH fraction showed an increase in the release of LDH in the cell culture medium with the lactate dehydrogenase activity of 52.3% and 61.6% at the GI_{50} and GI_{70} concentrations respectively with respect to the control. The apoptosis-inducing efficacy of the fraction was revealed by the damage and leakage caused by the loss of membrane potential as evaluated by LDH assay (Fig. 3).

Table 1 Phytochemical composition of CaFH fraction of *C. fistula* fruits as identified by HPLC analysis

Phytochemical	Peak (P)	Retention time (min)	Concentration (ppm)	Area/height (A/H)
Gallic acid	7	2.620	0.076	4.529
Catechin	12	3.968	1.516	7.741
Chlorogenic acid	13	4.640	0.289	7.071
Epicatechin	18	6.354	9.505	12.34
Caffeic acid	20	6.880	0.106	6.674
Umbelliferone	30	9.846	5.744	9.525
Coumaric acid	33	10.43	0.275	6.236
Rutin	44	14.99	0.798	7.788
Ellagic acid	46	15.69	10.61	9.274
Quercetin	48	16.66	2.832	9.609
Kaempferol	51	17.29	38.00	14.04

Confocal microscopy

Further experimentation was designed to unravel the mode of cancer cell death in human cervical cancer (HeLa) cell line treated with a fraction. The treatment of HeLa cells with different concentrations of CaFH (GI_{30} = 35.45 μg/ml, GI_{50} = 97.69 μg/ml, and GI_{70} = 269.2 μg/ml) fraction exhibited morphological changes like DNA fragmentation and chromatin condensation. The arrows indicate apoptotic bodies due to the formation of DNA fragments when apoptosis occurred in CaFH-treated cancer cells. In the case of untreated control cells, it was observed that the nucleus showed no sign of fragmentation and chromatin condensation (Fig. 4).

Scanning electron microscopy

The scanning electron microscopy (SEM) studies demonstrated that the treatment of HeLa cells with different concentrations (GI_{30}, GI_{50}, and GI_{70}) of CaFH fraction revealed various apoptotic features like membrane blebbing, shrinkage of cells, and formation of small apoptotic bodies. These morphological alterations demonstrated apoptosis as the formation of bubbles in the plasma membrane and condensation of chromatin, breaking the cancer cells and dividing it into apoptotic bodies. In the case of untreated control cells, it was observed that the cells showed intact morphology (Fig. 5).

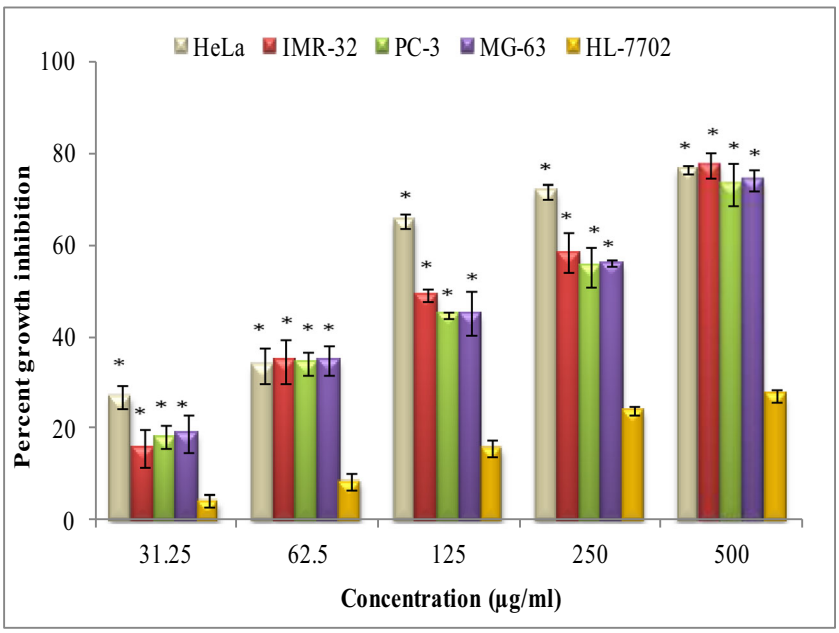

Fig. 1 HPLC chromatogram of CaFH fraction from *C. fistula* fruits

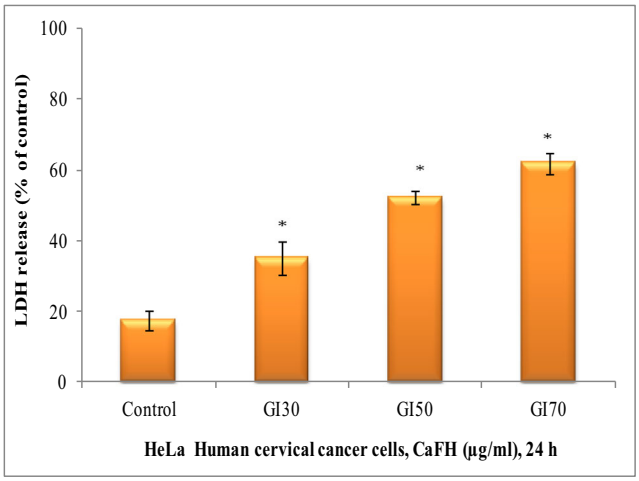

Fig. 2 Antiproliferative activity of CaFH from *C. fistula* fruits on different cell lines in MTT assay. Asterisk indicates statistically significant at $p \leq 0.05$

Cell cycle distribution

The cell proliferation is closely associated with the cell cycle. The apoptosis usually occurs when the cell cycle is arrested and cannot be restored. It was observed that in the CaFH fraction-treated cells, the percentage of G_0/G_1 phase of cell cycle gradually increased in a dose-dependent manner, whereas the percentage of S and G2/M phase was reduced. The CaFH fraction revealed enhancement in the arresting of the cell population at the G_0/G_1 phase of the cell cycle in HeLa cancer cells dose-dependently. The treatment of CaFH fraction caused the accumulation of cells by 50.2% in the G_0/G_1 phase at the maximum tested concentration (GI_{70}) in comparison to the untreated control as shown in Fig. 6.

Intracellular reactive oxygen species

The formation of reactive oxygen species (ROS) plays an essential role in the induction of apoptosis and

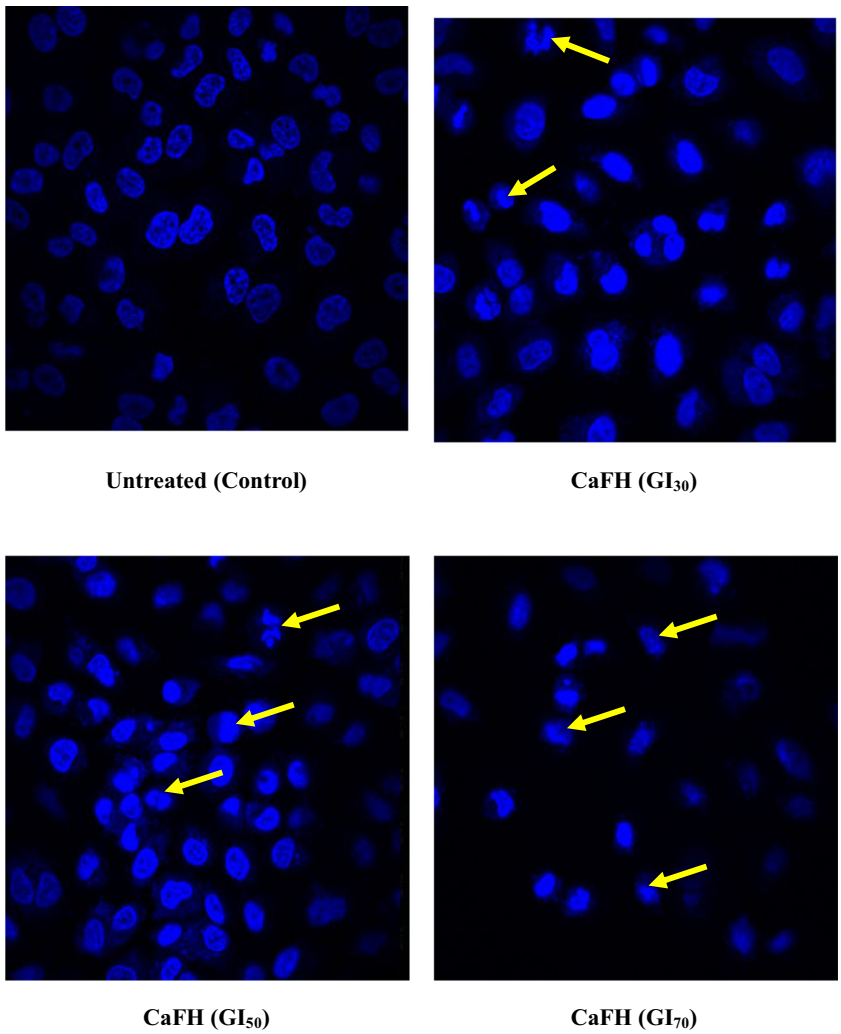

Fig. 3 Human cervical cancer (HeLa) cells were treated with different concentrations of CaFH from *C. fistula* fruits for 24 h through LDH assay. Asterisk indicates statistically significant at $p \leq 0.05$

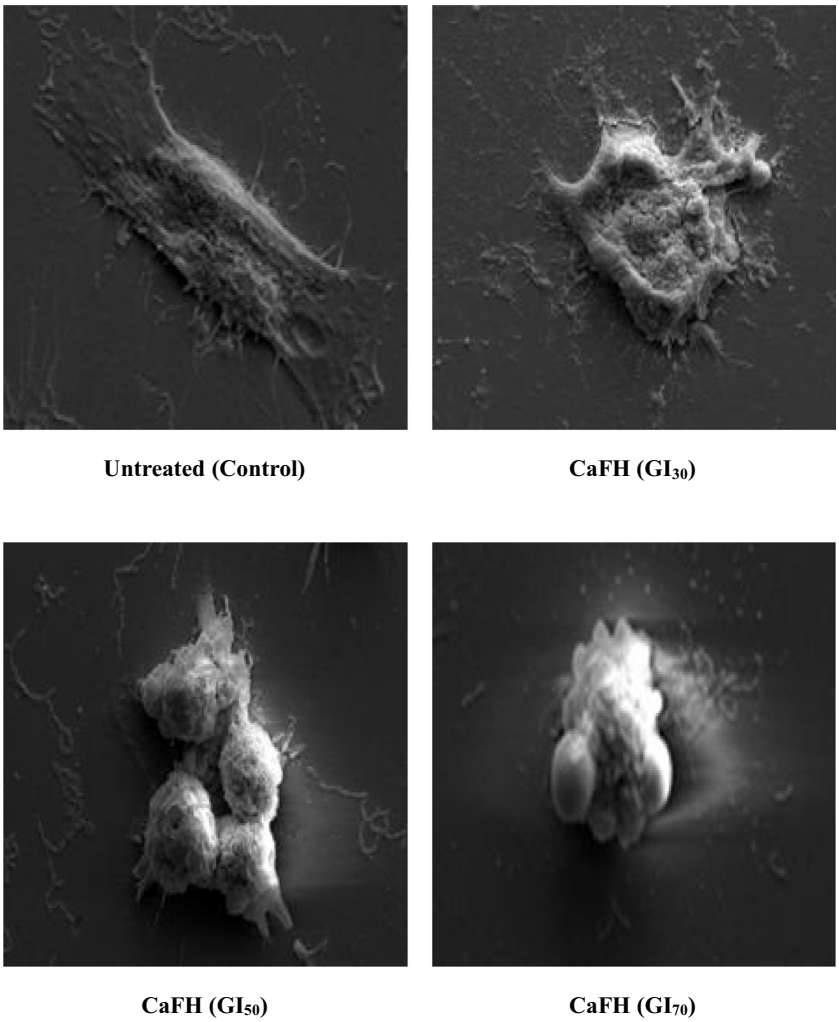

Fig. 4 Confocal micrographs of Hoechst 33342 stained HeLa cells treated with CaFH fraction from *C. fistula* for 24 h. Arrows shows DNA fragmentation, nuclear condensation, and formation of apoptotic bodies. Magnification × 60 oil immersion objective lens

mitochondria membrane depolarization. The intracellular ROS generation was measured by a non-fluorescent cell membrane permeable probe—2′,7′-dichlorofluorescein diacetate (DCFH-DA)—that is cleaved by non-specific cellular esterases/ROS and finally oxidized in the presence of peroxidases and H_2O_2 into the fluorescent 2′,7′-dichlorofluorescein (DCF). In this assay, M1 represents ROS negative that are real-time live cells, whereas M2 represents ROS positive that is a ROS display. The treatment of CaFH fraction exhibited enhancement in the proportion of (M2) ROS-positive group of cells in comparison to the untreated control cells in a dose-dependent manner. The CaFH fraction (GI_{30}, GI_{50}, and GI_{70} concentrations) treated HeLa cancer cells revealed an increase in the formation of ROS by 21.3%, 29.2%, and 36.5% in comparison to control cells as shown in Fig. 7. The level of DCF fluorescence in the cells treated with the fraction increased dose-dependently indicating the generation of ROS and demonstrated the induction of apoptosis.

Measurement of mitochondrial membrane potential ($\Delta\Psi m$)

Mitochondria play a key role in the apoptosis (intrinsic pathway) due to the involvement of membrane potential (Ψm) and the membrane permeability in the release of certain apoptogenic factors like cytochrome c and apoptosis-inducing factor (AIF) into the cytoplasm of the cell. To determine the changes in the mitochondrial membrane potential, it was observed that Rhodamine 123, a fluorescent probe, was used. In this, M1 represents the disruption in the mitochondrial membrane potential, whereas M2 represents the percentage of intact cells. It was found that the treatment of CaFH fraction showed an increase in the proportion of M1 cells demonstrating increased depolarized percentage resulting in the loss of mitochondrial membrane potential as compared to the untreated control cells in a dose-dependent manner. The treatment of CaFH fraction with different

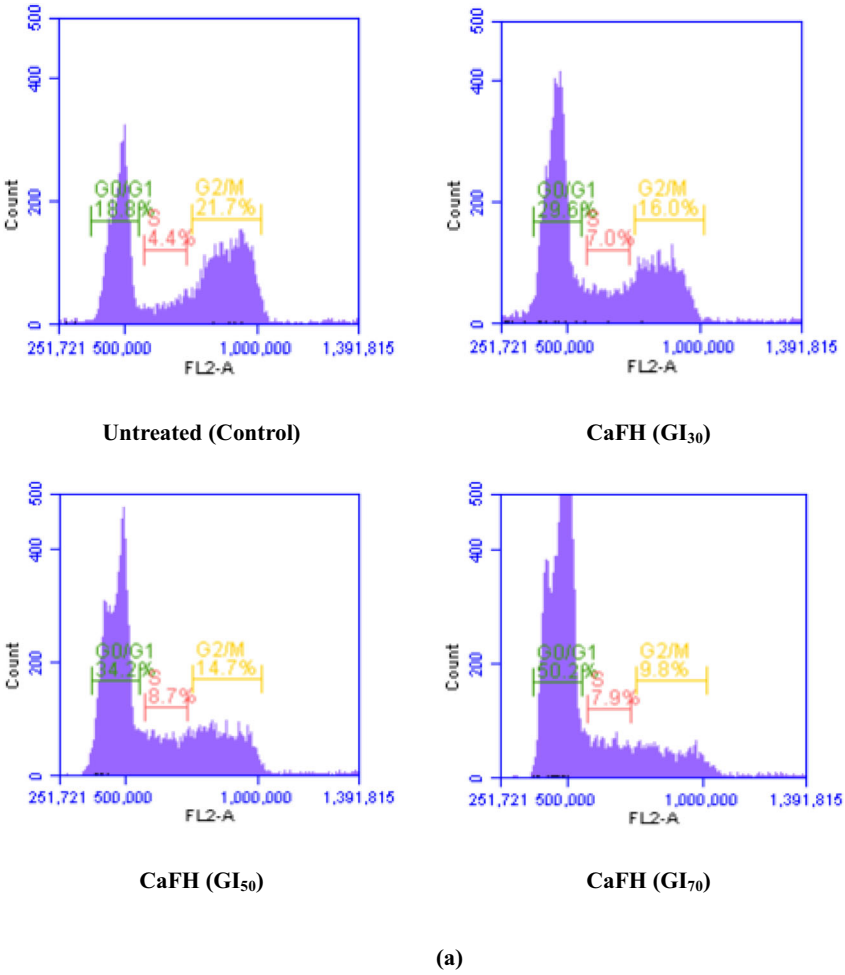

(a)

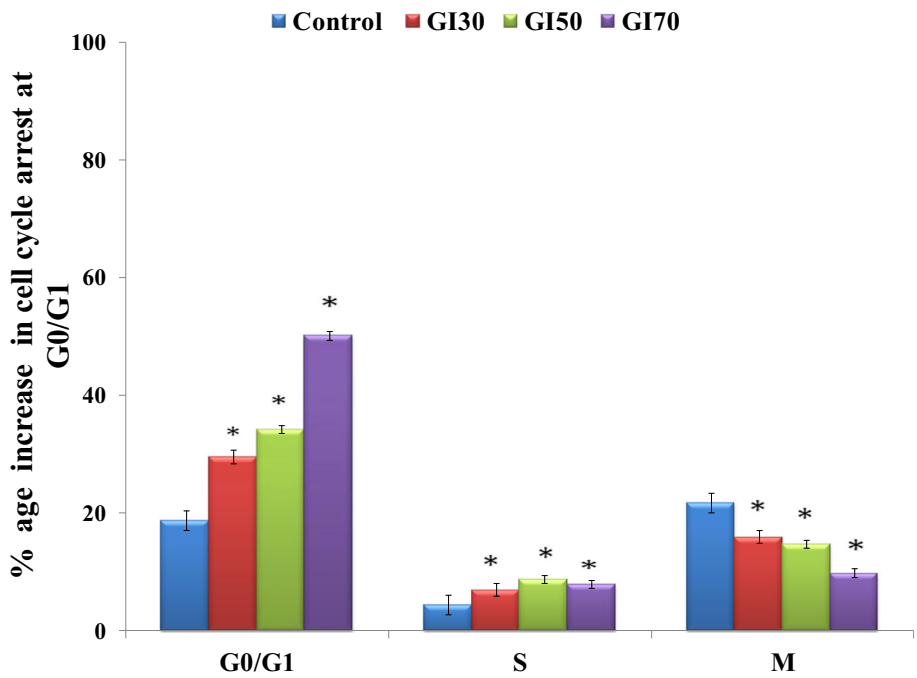

(b)

Fig. 5 Scanning electron micrographs (SEM) of HeLa cells before treatment shows intact cell and after treatment shows membrane blebbing with different concentrations of CaFH fraction from *C. fistula* (magnification 14 KX)

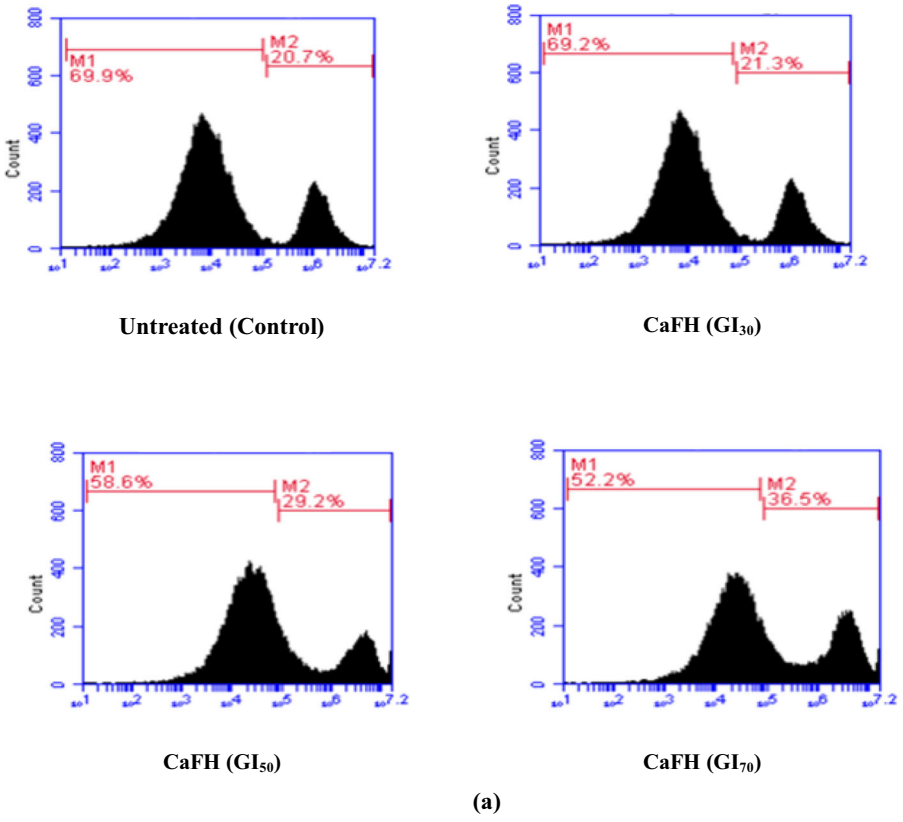

(a)

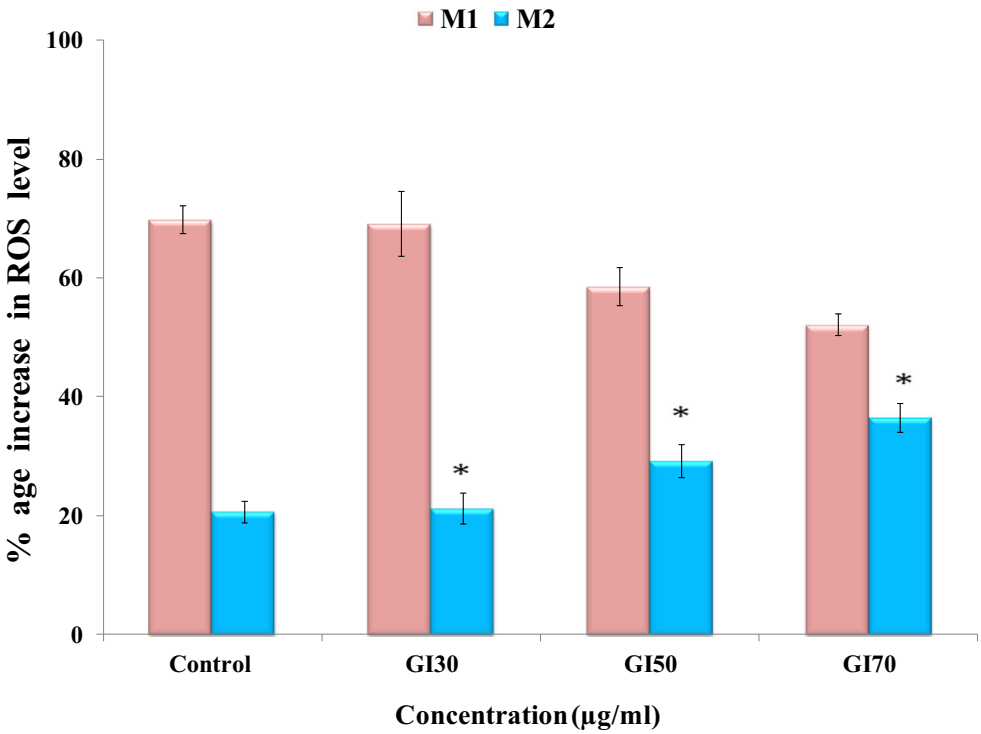

(b)

Fig. 6 **a** Effect on cell cycle analysis of HeLa cells treated with different concentrations of CaFH fraction from *C. fistula* for 24 h. For this, 20,000 events were acquired, cells were stained with PI and gated population analyzed using BD Accuri C6 flow cytometry to determine the DNA fluorescence. **b** Histograms showing that the values are expressed as mean ± SE. Asterisk indicates statistically significant at $p \leq 0.05$

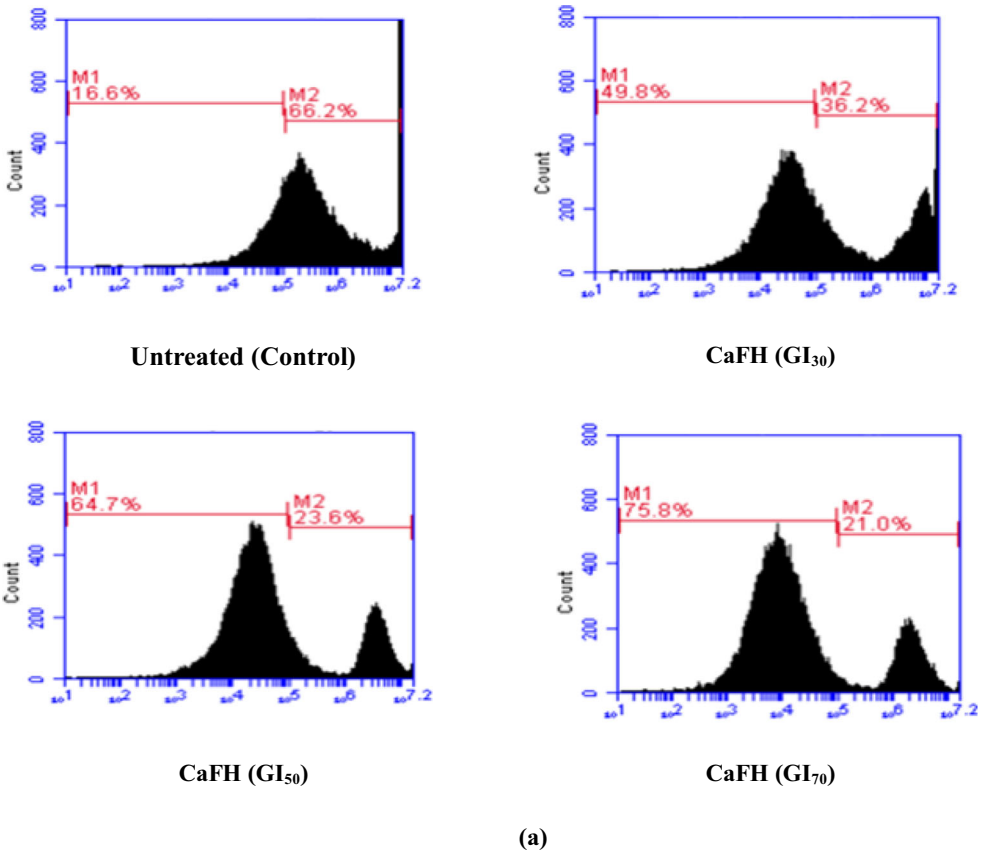

(a)

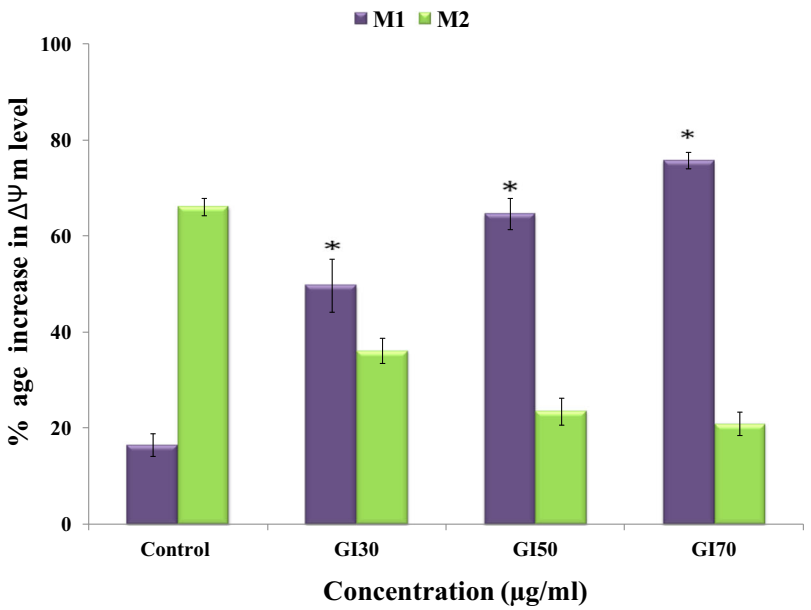

(b)

Fig. 7 **a** Effect of CaFH fraction from *C. fistula* on the generation of intracellular ROS in HeLa cells (24 h). DCFH-DA was used to stain the cells; 20,000 events were acquired and gated population analyzed using flow cytometer. M1 represents intact cell population and M2 represents cells with accumulation of intracellular ROS. **b** Histograms showing that the values are expressed as mean ± SE. Asterisk indicates statistically significant at $p \leq 0.05$

concentrations (GI_{30}, GI_{50}, and GI_{70}) showed an enhancement in the susceptibility of HeLa cancer cells' mitochondrial membrane depolarization by 49.8%, 64.7%, and 75.8% as compared to control (16.6%). The flow cytometric analysis revealed that the treatment with CaFH fraction showed a disruption in membrane

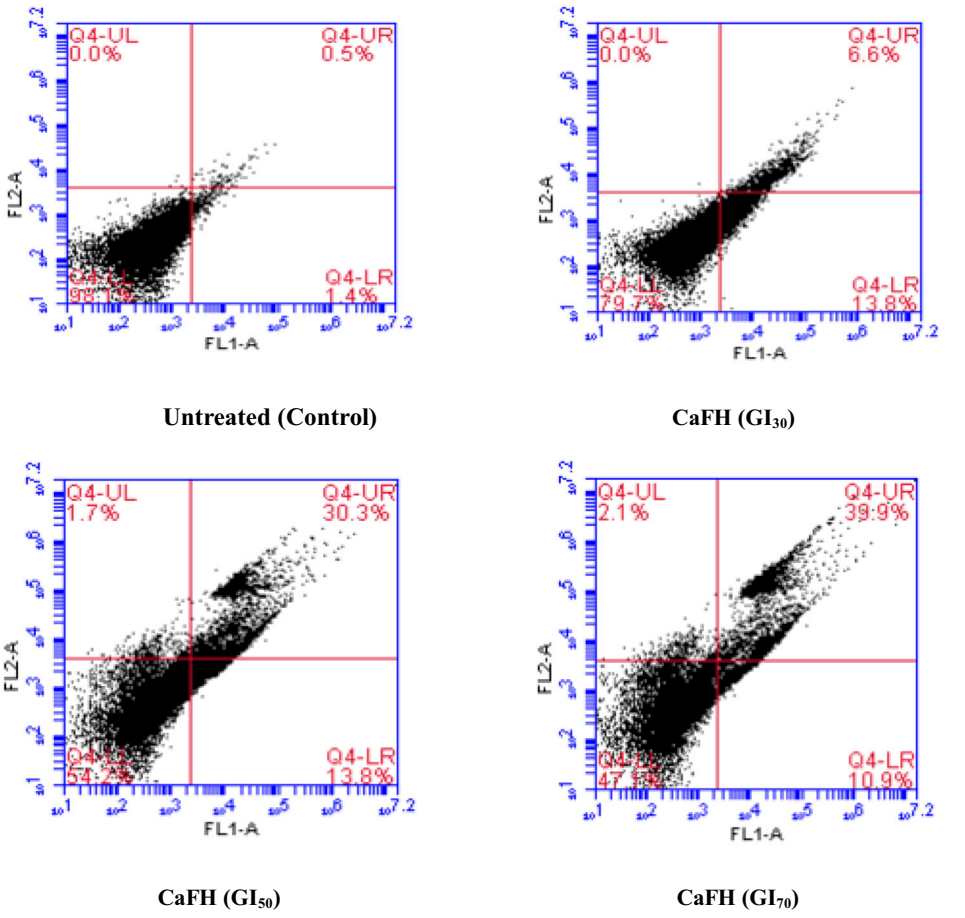

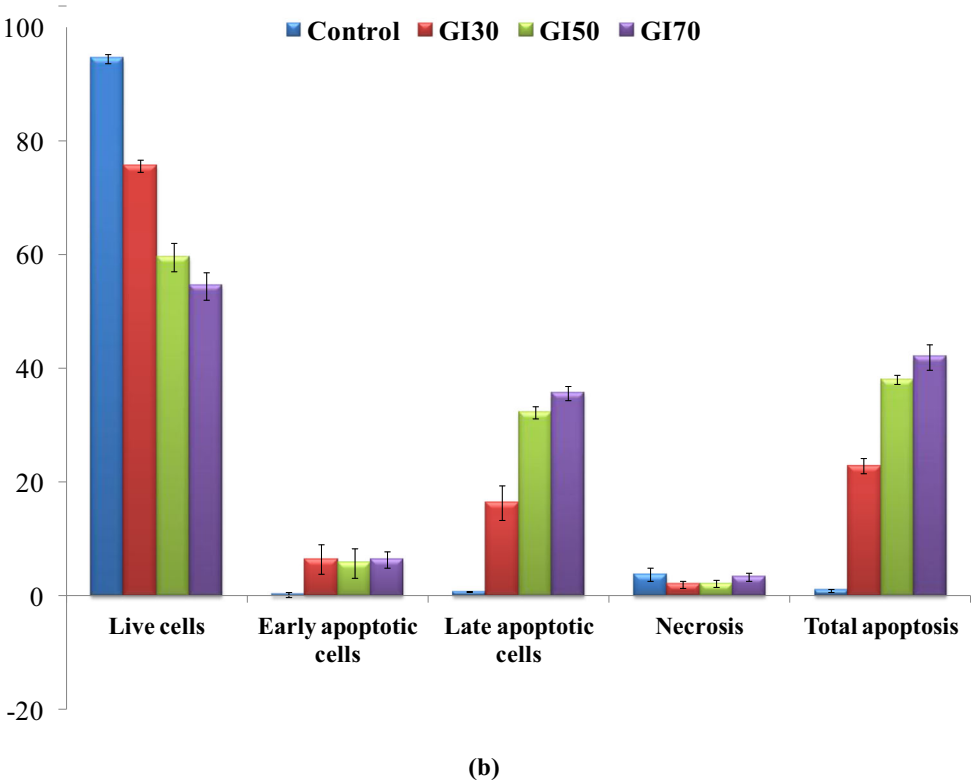

Fig. 8 **a** Effect of CaFH fraction from *C. fistula* on the disruption of mitochondrial membrane potential ($\Delta\Psi m$) in HeLa cells detected by staining with Rhodamine-123. For this, 20,000 events were acquired and gated population analyzed using flow cytometry. M1 represents cells with the disruption of $\Delta\Psi m$ and M2 represents the intact cells. **b** Histograms showing that the values are expressed as mean ± SE. Asterisk indicates statistically significant at $p \leq 0.05$

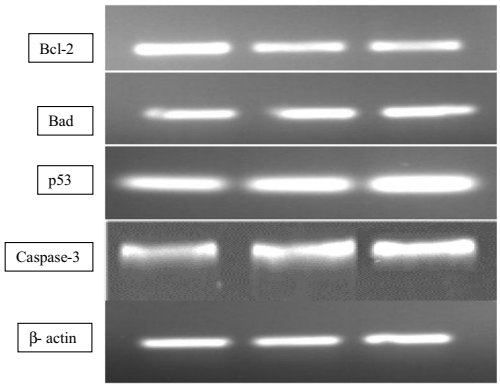

Fig. 9 **a** Effect of CaFH from *C. fistula* on cell apoptosis as detected by Annexin V-FITC/PI double staining in HeLa cells demonstrates the percentage of live cells (LL quadrant), early apoptotic cells (LR quadrant), late apoptotic cells (UR quadrant), and necrotic cells (UL quadrant). **b** Histograms showing that the values are expressed as Mean ± SE

potential of HeLa cells dose-dependently after 24 h as depicted in Fig. 8.

Annexin V-FITC/PI double staining

The apoptotic cell population demonstrated an increase in CaFH fraction-treated HeLa cells by 20.4%, 44.1%, and 50.8% (both early and late apoptotic cells population) in comparison with untreated control cells. The apoptotic mode of cell death was observed by the externalization of phosphatidylserine to the cell surface indicating an increase in the percentage of cells in the early and late apoptotic phases. The results obtained showed that the treatment of CaFH fraction significantly suppressed the growth of human cervical cancer HeLa cells through the induction of apoptosis in a dose-dependent manner (Fig. 9).

Semi-quantitative RT-PCR

For determining the molecular changes in gene expression level related to apoptosis, the effect of CaFH fraction-treated human cervical cancer HeLa cells was investigated on the expression of genes such as Bcl-2, p53, Bad, and caspase-3 by semi-quantitative RT-PCR. The molecular changes in the CaFH fraction-treated cells and negative control cells were analyzed. It was found that the cells treated with different concentrations (GI_{50} and GI_{70}) of n-hexane fraction exhibited a decrease in the gene expression level of the Bcl-2 gene and an increase in the expression level of p53, Bad, and caspase-3 genes as analyzed using semi-quantitative RT-PCR. Furthermore, the data obtained revealed that the CaFH induce apoptosis through Bcl-2 suppression and the activation of p53 and Bad. The expression of caspase-3 was increased as compared to the untreated control to confirm the final stage of apoptosis (Fig. 10).

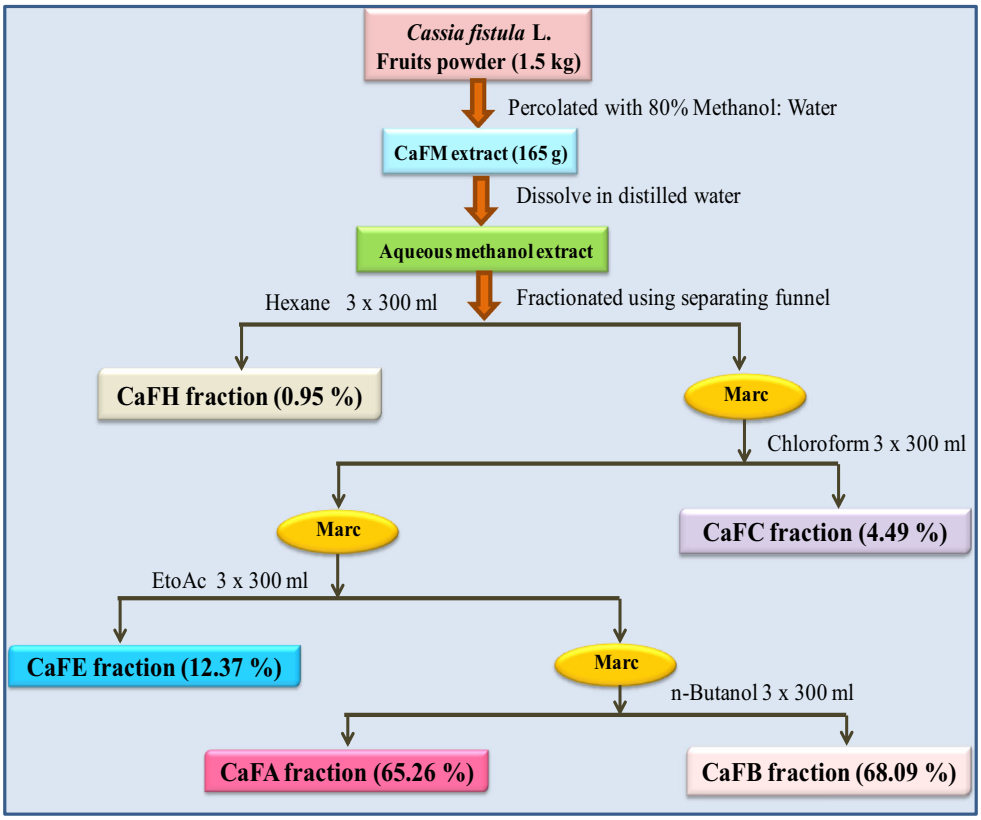

Fig. 10 Semi-quantitative RT-PCR analysis demonstrated that n-hexane fraction regulates the expression of various genes involved in cellular signaling pathways for the induction of apoptosis in HeLa cancer cells. (lane 1: control; lane 2: GI-50 of CaFH; lane 3: GI-70 of CaFH)

Discussion

Phytochemicals derived from plants act as secondary plant metabolites that play a crucial role in cancer chemoprevention by inhibiting the ROS-scavenging system to induce oxidative stress-mediated cell death, activating apoptosis-related signals, and suppressing the pro-survival signals favoring the growth of cancer cells (Chikara et al. 2018). In the current study, the antiproliferative and pro-apoptotic potentials of n-hexane (CaFH) fraction from *C. fistula* fruits were investigated. The cytotoxicity of the CaFH fraction was evaluated against a panel of cancer cell lines, namely HeLa (human cervical cancer), IMR-32 (human neuroblastoma), PC-3 (human prostate adenocarcinoma), MG-63 (human osteosarcoma) cell lines, along with normal HL-7702 (human hepatocyte) cell line using MTT assay. The HPLC profiling of CaFH fraction indicated the presence of Kaempferol, Ellagic acid, and Epicatechin in the appreciable amount (Fig. 1 and Table 1). CaFH fraction exhibited the lowest GI_{50} value of 97.69 μg/ml in the HeLa cancer cell line as compared to other cell lines and was observed to be ineffective toward HL-7702 normal cell line (Fig. 2). In the current study, it was evaluated that the antiproliferative activity of the fraction effectively suppressed the activity of mitochondrial succinate dehydrogenase enzyme that undergoes the conversion of soluble MTT dye into insoluble formazan. Uesato et al. (2001) evaluated the growth inhibitory effects of green tea catechins namely (−)-epicatechin (EC), (−)-epigallocatechin (EGC), and (−)-epigallocatechin gallate (EGCG) in the HCT 116 colorectal and HepG2 hepatocellular carcinoma cell lines. It was found that EGC and EGCG showed the lowest IC_{50} of 7.6 ± 0.4 and 11.2 ± 0.5 μM against the HCT 116 cell line in MTT assay. A study reported the antiproliferative effects of Kaempferol against a panel of human cancer cell lines including human breast carcinoma (MCF-7) cells, human lung carcinoma (A549) cells, human stomach carcinoma (SGC-7901) cells, and human cervical carcinoma (HeLa) cells (Liao et al. 2016). Lactate dehydrogenase, a marker of membrane leakage/damage demonstrating apoptotic mode of cell death, was further evaluated by the increase in the release of LDH in the culture medium of the HeLa cells treated with the various concentrations of CaFH fraction (Fig. 3). It was found that cancer cells showed a high rate of glycolysis for survival. There is a direct conversion of pyruvate into lactate with the help of lactate dehydrogenase enzyme, instead of entering into the citric acid cycle. This step produces NAD^+ and consumes NADH, resulting in the reduction of mitochondrial membrane potential and induction of apoptosis (Franco-Molina et al. 2010).

In the treatment of cancer, phytochemicals showed enhancement in the level of oxidative stress in cancer cells by inducing DNA damage, inactivating the growth signals, suppression of the ROS-scavenging system, induction of apoptosis-related signals, and targeting the signaling pathways that favor the growth of cancer cells. The major feature of many types of cancer is the evasion of cells from apoptosis (Reed 2003). The anticancer properties of chemopreventive agents can restore the normal apoptotic functioning of cellular proteins. In the current study, it was observed that the CaFH fraction demonstrated the effectiveness in inhibiting the growth of the human cervical cancer HeLa cells and was further explored for the induction of apoptosis as one of the major mechanisms of cell death. CaFH fraction exhibited certain cellular morphological alterations such as shrinkage of the cell, DNA fragmentation, membrane blebbing, the formation of apoptotic bodies, and chromatin condensation as revealed by confocal and SEM microscopy (Figs. 4 and 5). *Stryphnodendron adstringens* (barbatimão) leaf aqueous extract treatment revealed morphological changes like rounding-up, cell shrinkage, nuclear condensation, and decrease in length and diameter of cell in two human breast carcinoma cell lines like MDA-MB-435 and MCF-7. The fraction was found to be a rich source of (−)-epicatechin-3-O-gallate, procyanidin dimer B1, and gallic acid (Sabino et al. 2018).

The cell cycle arrest is directly related to apoptosis and normally occurs due to the activation of the p53 tumor suppressor gene serving as an important target in cancer therapy. The CaFH fraction was observed to cause the accumulation of cell population at the G_0/G_1 phase of the cell cycle which inhibited the growth of HeLa cancer cells, and this activity might be attributed to the presence of effective phytoconstituents in it. The fraction exhibited the arresting of cells at the percentage of 29.6%, 34.2%, and 50.2% at different tested concentrations (Fig. 6). Yu et al. (2015) reported the anticarcinogenic effects of umbelliferone isolated from *Ferula communis* against HepG2 hepatocellular carcinoma cell line. A study has found (Ho et al. 2014) that Ellagic acid promotes cytotoxicity, arrest the cells at the G0/G1 phase, and induced apoptosis in human bladder cancer TSGH8301 cells by enhancing the expression level of p53, p21, BAD, cytochrome c, AIF, and cleavage of caspases 9 and 3 while reducing the level of Cdc2 and Wee1. Choi and Ahn (2008) evaluated that the exposure of kaempferol at the dose of 10 and 50 μM resulted in growth inhibition and cell cycle arresting at the G2/M phase in human breast cancer MDA-MB-453 cells. It was also demonstrated that the induction of apoptosis is strongly associated with the arresting of the cell cycle.

The enhancement of reactive oxygen species (ROS) generation in cancer cells is found to be an efficient mechanism for the induction of apoptosis using the compound 2′,7′-dichlorodihydrofluorescein diacetate (DCFH-DA). The CaFH fraction showed an increase in the intracellular ROS formation by 21.3% > 29.2% > 36.5% as expressed by the M2 cell population in the DCFH-DA-stained HeLa cells analyzed using flow cytometer in a dose-dependent manner (Fig. 7). Wei et al. (2018) reported that Xanthohumol, a prenylated flavonoid isolated from *Humulus lupulus* L.,

showed antiproliferative and apoptotic properties in gastric cancer AGS cells by the overproduction of ROS. The cytotoxicity and apoptosis-inducing potential of Kaempferol was evaluated in colorectal cancer HCT116 cells and showed an increase in the level of ROS generation (Choi et al. 2018).

The disruption in the mitochondrial membrane permeability is an essential feature for determining apoptosis in cancer cells. However, in the case of apoptotic cells with disruption of their membrane integrity, no accumulation of Rhodamine-123 occurs as the dye can freely move inside and outside the mitochondria. The CaFH fraction showed a decrease in Rhodamine fluorescence intensity by 64.7% at the GI_{50} concentration pointing toward the decrease in mitochondrial membrane potential ($\Delta\Psi m$) in HeLa cancer cells (Fig. 8). The aqueous extract containing epigallocatechin, gallocatechin, gallic acid, and dimeric and trimeric proanthocyanidins from *Stryphnodendron adstringens* stem bark showed potent anticancer effects by the induction of mitochondrial membrane potential dysfunction in murine B16F10Nex-2 melanoma cells (Baldivia et al. 2018). Kaempferol showed the antiproliferative and apoptosis-inducing potential by causing mitochondrial membrane depolarization in the human glioma cells in a dose- and time-dependent manner (Jeong et al. 2009).

The apoptosis-inducing capacity of the fraction was analyzed by the phosphatidylserine (PS) externalization that leads to the translocation of PS from the inner to the outer leaflet of the plasma membrane in Annexin V-FITC/PI double staining analyzed using flow cytometry. The CaFH fraction-treated HeLa cancer cells showed enhancement in the level of an apoptotic cell population by 44.1% and 50.8% at the GI_{50} and GI_{70} concentrations analyzed using Annexin-V/PI double staining assay (Fig. 9). Chuwa et al. (2018) reported the modulation of mitochondrial pathway and/or death receptor pathway by Kaempferol, a bioflavonoid through the induction of apoptosis in ER-positive endometrial cancer cell lines as detected by Annexin V-FITC/PI double staining. The methanol extract and its n-hexane fraction extracted from *Ziziphus obtusifolia* causes induction in the phosphatidylserine externalization and thereby increases the early apoptotic cells percentage from untreated control cells (1.4%) to 1.9% and 3.5% for both the methanol extract and n-hexane fraction-treated cells, respectively (Molina-Romo et al. 2018).

The pro-survival Bcl-2 (B cell lymphoma 2) family gene expression facilitates tumorigenesis through the resistance of apoptotic cell death (Hockenbery et al. 1990; Campbell and Tait 2018). Bad (Bcl-2 agonist of cell death) is a pro-apoptotic protein and BH3-only member that regulates apoptosis (Engel and Henshall 2009; Bui et al. 2018). In the present study, it was found that CaFH fraction from *C. fistula* fruits suppressed the activation of the Bcl-2 gene while it promotes upregulation in the expression of apoptosis-inducing gene, Bad in HeLa cancer cells (Fig. 10). Quercetin is reported to upregulate the expression of pro-apoptotic proteins (Bax and Bad) and downregulate the level of anti-apoptotic proteins, Bcl-2 and Bcl-xl, thereby suppressing cell proliferation and promoting the induction of apoptosis in various cancer cell lines (Vijayababu et al. 2005; Zhang et al. 2012; Deng et al. 2013). p53 is a transcription factor that activates in response to DNA damage which led to cell growth arrest, allowing DNA repair and cellular apoptosis to maintain the integrity of genome (Mijit et al. 2020). CaFH fraction was found to induce apoptosis by upregulating the expression level of p53 analyzed using semi-quantitative RT-PCR (Fig. 10). Fu et al. (2017) reported that flavonoids and tannins from *Smilax china* L. rhizome showed the inhibition of cell proliferation and induction of apoptosis in human lung adenocarcinoma A549 cells by upregulating the p53 expression level. Narayanan and Re (2001) demonstrated the anticarcinogenic effects of ellagic acid against the growth and proliferation of colon cancer (SW 480) cells. The treatment of Ellagic acid caused G_1 and S phase cell cycle arrest which was further accompanied by the activation of p53. Caspases are endoproteases that play a crucial role in maintaining the homeostasis through the regulation of inflammation and cell death. The executioner caspases (caspase-3, -6, and -7) confirm and control the final step of apoptosis (McIlwain et al. 2013). The growth inhibitory effect of CaFH fraction was further accompanied by the activation of caspase-3, an important marker of the apoptotic mode of cell death (Fig. 10). It was found that Kaempferol showed its antiproliferative and apoptosis-inducing properties on human ovarian cancer OVACAR-3 cells by upregulating the expression level of caspase 3 (Yang et al. 2019). Taken together, the outcome of the CaFH fraction-treated cells demonstrated its anticancer efficacy through the inhibition of cell proliferation and promotion of the pro-apoptotic activity.

Conclusion

The data obtained demonstrated that CaFH fraction suppressed the proliferation of human cervical cancer HeLa cells by the induction of apoptosis. This apoptotic effect might be attributed to the pro-oxidant properties of the phytoconstituents present in the CaFH fraction. This was evident by morphological alterations, G0/G1 phase cell cycle arrest, decreased MMP level, increased ROS level, and Annexin V-positive cell population. CaFH fraction induced apoptosis by downregulating the expression of anti-apoptotic Bcl-2 gene, whereas it upregulates the expression of pro-apoptotic, Bad, caspase-3, and p53, genes in HeLa cells. The above results deciphered in the present study point toward its ability to inhibit the growth and development of cervical cancer thereby proving its prospective use as a cancer chemopreventive agent.

Acknowledgments We are grateful to the Indian Council of Medical Research (ICMR) [59/36/2011/BMS/TRM], New Delhi (India) and Centre of Emerging Life Sciences, Guru Nanak Dev University, Amritsar (India) for providing the necessary facilities and support.

Author's contribution Drafted the manuscript and supervised with her personal inputs: S.K and S.J.K. Methodology and reviewed the literature: S.K., K.P, and M.C. Statistical analysis of the results, interpretation of data: S.K., and K.P. Interpretation and data validation: S.K and S.J.K; gene expression analysis: S.K.

Compliance with ethical standards

Conflict of interest The authors declare that they have no conflict of interest.

References

Abe K, Matsuki, N (2000) Measurement of cellular 3-(4,5-dimethylthiazol-2-yl)-2,5-diphenyl- tetrazolium bromide (MTT) reduction activity and lactate dehydrogenase release using MTT. Neurosci Res 38:325–329.

Baldivia DDS, Leite DF, Castro DTH, Campos JF, Santos UPD, Paredes-Gamero EJ, Carollo CA, Silva DB, de Picoli SK, Dos Santos EL (2018) Evaluation of *in vitro* antioxidant and anticancer properties of the aqueous extract from the stem bark of *Stryphnodendron adstringens*. Int J Mol Sci 19(8). https://doi.org/10.3390/ijms19082432

Bhalerao SA, Kelkar TS (2012) Traditional medicinal uses, phytochemical profile and pharmacological activities of *Cassia fistula* Linn. Internet Res 1(5):79–84

Bui NL, Pandey V, Zhu T, Ma L, Basappa LPE (2018) Bad phosphorylation as a target of inhibition in oncology. Cancer Lett 415:177–186. https://doi.org/10.1016/j.canlet.2017.11.017

Campbell KJ, Tait SWG (2018) Targeting BCL-2 regulated apoptosis in cancer. Open Biol 8:180002. https://doi.org/10.1098/rsob.180002

Carino-Cortes R, Hernández-Ceruelos A, Torres-Valencia JM, González-Avila M, Arriaga-Alba M, Madrigal-Bujaidar E (2007) Antimutagenicity of *Stevia pilosa* and *Stevia eupatoria* evaluated with the Ames test. Toxicol in Vitro 21:691–697

Chen M, Sun X, Wang Y, Ling K, Chen C, Cai X, Liang X, Liang Z (2019) FAT1 inhibits the proliferation and metastasis of cervical cancer cells by binding β-catenin. Int J Clin Exp Pathol 12(10):3807–3818

Chikara S, Nagaprashantha LD, Singhal J, Horne D, Awasthi S, Singhal SS (2018) Oxidative stress and dietary phytochemicals: role in cancer chemoprevention and treatment. Cancer Lett 413:122–134

Choi EJ, Ahn WS (2008) Kaempferol induced the apoptosis via cell cycle arrest in human breast cancer MDA-MB-453 cells. Nutr Res Pract 2(4):322–325

Choi JB, Kim JH, Lee H, Pak JN, Shim BS, Kim SH (2018) Reactive oxygen species and p53 mediated activation of p38 and caspases is critically involved in Kaempferol induced apoptosis in colorectal cancer cells. J Agric Food Chem 66(38):9960–9967

Chuwa AH, Sone K, Oda K, Tanikawa M, Kukita A, Kojima M, Oki S, Fukuda T, Takeuchi M, Miyasaka A, Kashiyama T, Ikeda Y, Nagasaka K, Mori-Uchino M, Matsumoto Y, Wada-Hiraike O, Kuramoto H, Kawana K, Osuga Y, Fujii T (2018) Kaempferol, a natural dietary flavonoid, suppresses 17β-estradiol-induced survivin expression and causes apoptotic cell death in endometrial cancer. Oncol Lett 16(5):6195–6201

Deng XH, Song HY, Zhou YF, Yuan GY, Zheng FJ (2013) Effects of quercetin on the proliferation of breast cancer cells and expression of survivin *in vitro*. Exp Ther Med 6:1155–1158

Duraipandiyan V, Arul AB, Ignacimuthu S, Muthukumar C, Al-Harbi NA (2012) Anticancer activity of Rhein isolated from *Cassia fistula* L. flower. Asian Pac. J. Trop. Dis. 2(1):517–523

Engel T, Henshall DC (2009) Apoptosis, Bcl-2 family proteins and caspases: the ABCs of seizure-damage and epileptogenesis? IJPPP 1:97–115

Inkabi SE, Larbie C (2017) Review of Some ornamental plants used in the treatment of reproductive disorders. IJPPR. 9(1):1-9

Franco-Molina MA, Mendoza-Gamboa E, Sierra-Rivera CA, Gómez-Flores RA, Zapata-Benavides P, Castillo-Tello P, Alcocer-González JM, Miranda-Hernández DF, Tamez-Guerra RS, Rodríguez-Padilla C (2010) Antitumor activity of colloidal silver on MCF-7 human breast cancer cells. J Exp Clin Cancer Res 29(1):148. https://doi.org/10.1186/1756-9966-29-148

Fu S, Yang Y, Liu D, Luo Y, Ye X, Liu Y, Chen X, Wang S, Wu H, Wang Y, Hu Q, You P (2017) Flavonoids and tannins from *Smilax china* L. rhizome induce apoptosis via mitochondrial pathway and MDM2-p53 signaling in human lung adenocarcinoma cells. Am J Chin Med 45(2):369–384

Gomes IZF, Silva-Oliveira RJ, Silva VAO, Rosa MN, Vital PS, Barbosa MCS, Santos FVD, Junqueira JGM, Severino VGP, Oliveira BG, Romao W, Reis RM, Ribeiro RIMDA (2019) *Annona coriacea* Mart. fractions promote cell cycle arrest and inhibit autophagic flux in human cervical cancer cell lines. Molecules 24(1):3963

Gupta UC, Jain GC (2009) Study on hypolipidemic activity of *Cassia fistula*. legume in rats. Asian J Exp Sci 23(1):241–248

Hanahan D, Weinberg RA (2000) The hallmarks of cancer. Cell 100(1):57–70

Ho CC, Huang AC, Yu CS, Lien JC, Wu SH, Huang YP, Huang HY, Kuo JH, Liao WY, Yang JS, Chen PY, Chung JG (2014) Ellagic acid induces apoptosis in TSGH8301 human bladder cancer cells through the endoplasmic reticulum stress- and mitochondria-dependent signaling pathways. Environ Toxicol 29(11):1262–1274

Hockenbery D, Nunez G, Milliman C, Schreiber RD, Korsmeyer SJ (1990) Bcl-2 is an inner mitochondrial membrane protein that blocks programmed cell death. Nature 348:334–336

Jeong JC, Kim MS, Kim TH, Kim YK (2009) Kaempferol induces cell death through ERK and Akt-dependent down-regulation of XIAP and survivin in human glioma cells. Neurochem Res 34(5):991–1001

Kotecha R, Takami A, Espinoza JL (2016) Dietary phytochemicals and cancer chemoprevention: a review of the clinical evidence. Oncotarget 7(32):52517–52529

Liao W, Chen L, Ma X, Jiao R, Li X, Wang Y (2016) Protective effects of kaempferol against reactive oxygen species-induced hemolysis and its antiproliferative activity on human cancer cells. Eur J Med Chem 114:24–32

McIlwain DR, Berger T, Mak TW (2013) Caspase functions in cell death and disease. Cold Spring Harb Perspect Biol 5:a008656

Mickisch G, Fajta S, Keilhauer G, Schlike E, Tschada P, Alken P (1990) Chemosensitivity testing of primary human renal cell carcinoma by tetrazolium based microculture assay (MTT). Urol Res 18:131–136

Mijit M, Caracciolo V, Melillo A, Amicarelli F, Giordano A (2020) Role of p53 in the regulation of cellular senescence. Biomolecules 10(3). https://doi.org/10.3390/biom10030420

Militao GCG, Dantas INF, Pessoa C, Falcão MJC, Silveira ER, Lima MAS, Curi R, Lima T, Moraes MO, Costa-Lotufo LV (2006)

Induction of apoptosis by pterocarpans from *Platymiscium floribundum* in HL-60 human leukemia cells. Life Sci 78:2409–2417

Molina-Romo ED, Garibay-Escobar A, Valenzuela-Antelo O, Ruiz-Bustos E, Martínez JH, Vélazquez C, Rascón-Valenzuela LA, Robles-Zepeda RE (2018) Antiproliferative and apoptotic activities of the medicinal plant *Ziziphus obtusifolia*. Pharm Res 10(1):55–59. https://doi.org/10.4103/pr.pr_38_17

Moradi-Afrapoli F, Shokrzadeh M, Barzegar F, Gorji-Bahri G, Zadali R, Ebrahim SN (2018) Cytotoxic activity of abietane diterpenoids from roots of *Salvia sahendica* by HPLC-based activity profiling. Rev Bras Farmacogn 28(1):27–33

Muntean DM, Sturza A, Pavel IZ, Duicu OM (2018) Modulation of cancer metabolism by phytochemicals—a brief overview. Anti Cancer Agents Med Chem 18(5):684–692

Narayanan BA, Re GG (2001) IGF-II down regulation associated cell cycle arrest in colon cancer cells exposed to phenolic antioxidant ellagic acid. Anticancer Res 21(1A):359–364

Neergheen VS, Bahorun T, Taylor EW, Jen LS, Aruoma OI (2010) Targeting specific cell signaling transduction pathways by dietary and medicinal phytochemicals in cancer chemoprevention. Toxicology 278(2):229–241

Preethy CP, Padmapriya R, Periasamy VS, Riyasdeen A, Srinag S, Kishnamurthy H, Alshatwi AA, Akbarsha MA (2012) Antiproliferative property of n-hexane and chloroform extracts of *Anisomeles malabarica* (L). R. Br. In HPV16-positive human cervical cancer cells. J Pharmacol Pharmacother 3(1):26–34

Priyadarsini RV, Nagini S (2012) Cancer chemoprevention by dietary phytochemicals: promises and pitfalls. Curr Pharm Biotechnol 13:125–136

Rather RA, Bhagat M (2018) Cancer chemoprevention and piperine: molecular mechanisms and therapeutic opportunities. Front Cell Dev Biol 6(10):1–12. https://doi.org/10.3389/fcell.2018.00010

Reed JC (2003) Apoptosis-targeted therapies for cancer. Cancer Cell 3(1):17–22

Reyes-Lopez M (2005) The amoebicidal aqueous extract from *Castela texana* possesses antigenotoxic and antimutagenic properties. Toxicol in Vitro 19:91–97

Riyasdeen A, Periasamy VS, Paul P, Alshatwi A A, Akbarsha MA (2012). Chloroform extract of Rasagenthi Mezhugu, a siddha formulation, as an evidence-based complementary and alternative medicine for HPV-positive cervical cancers. Evid Based Complement Alternat Med. 136527

Sabino APL, Eustáquio LMS, Miranda ACF, Biojone C, Mariosa TN, Gouvêa CMCP (2018) *Stryphnodendron adstringens* ("Barbatimão") leaf fraction: chemical characterization, antioxidant activity, and cytotoxicity towards human breast cancer cell lines. Appl Biochem Biotechnol 184(4):1375–1389

Saei Ghare Naz M, Kariman N, Ebadi A (2018) Educational interventions for cervical cancer screening behavior of women: a systematic review. Asian Pac J Cancer Prev 19:875–884

Salehi B, Zucca P, Sharifi-Rad M, Pezzani R, Rajabi S, Setzer WN, Varoni EM, Iriti M, Kobarfard F, Sharifi-Rad J (2018) Phytotherapeutics in cancer invasion and metastasis. Phytother Res 32(8):1425–1449. https://doi.org/10.1002/ptr.6087

Shu L, Cheung K-L, Khor TO, Chen C, Kong A-N (2010) Phytochemicals: cancer chemoprevention and suppression of tumor onset and metastasis. Cancer Metastasis Rev 29:483–502

Torre LA, Bray F, Siegel RL, Ferlay J, Lortet-Tieulent J, Jemal A (2015) Global cancer statistics, 2012. CA Cancer J Clin 65:87–108

Uesato S, Kitagawa Y, Kamishimoto M, Kumagai A, Hori H, Nagasawa H (2001) Inhibition of green tea catechins against the growth of cancerous human colon and hepatic epithelial cells. Cancer Lett 170:41–44

Vijayababu M, Kanagaraj P, Arunkumar A, Ilangovan R, Aruldhas M, Arunakaran J (2005) Quercetin-induced growth inhibition and cell death in prostatic carcinoma cells (PC-3) are associated with increase in p21 and hypophosphorylated retinoblastoma proteins expression. J Cancer Res Clin 131:765–771

Wei S, Sun T, Du J, Zhang B, Xiang D, Li W (2018) Xanthohumol, a prenylated flavonoid from hops, exerts anticancer effects against gastric cancer in vitro. Oncol Rep 40(6):3213–3222

Yang S, Si L, Jia Y, Jian W, Yu Q, Wang M, Lin R (2019) Kaempferol exerts anti-proliferative effects on human ovarian cancer cells by inducing apoptosis, G_0/G_1 cell cycle arrest and modulation of MEK/ERK and STAT3 pathways. J BUON 24(3):975–981

Yessaian A, Magistris A, Burger RA, Monk BJ (2004) Radical hysterectomyfollowed by tailored postoperative therapy in the treatment of stage IB2 cervical cancer: feasibility and indications for adjuvant therapy. Gynecol Oncol 94:61–66

Yu SM, Hu DH, Zhang JJ (2015) Umbelliferone exhibits anticancer activity via the induction of apoptosis and cell cycle arrest in Hep G2 hepatocellular carcinoma cells. Mol Med Rep 12(3):3869–3873

Zhang H, Zhang M, Yu ZY, He N, Yang X (2012) Antitumor activities of quercetin and quercetin-5′,8-disulfonate in human colon and breast cancer cell lines. Food Chem Toxicol 50:1589–1599

Zhang J, Sia J, Gan L, Guo M, Yan J, Chen Y, Wang F, Xie Y, Wang Y, Zhang H (2020) Inhibition of Wnt signalling pathway by XAV939 enhances radiosensitivity in human cervical cancer HeLa cells. Artif Cells Nanomed Biotechnol 48:479–487